Ph. D. Thesis

Synchronized oscillatory discharges of mitral/tufted cells and olfactory information processing in the MOB

Hideki Kashiwadani

Department of Biophysical Engineering
Faculty of Engineering Science
Osaka University
Toyonaka, Osaka 560-8531, Japan.

Abstract

Central olfactory system integrates signals derived from numerous types of odorant receptors that are expressed by sensory neurons in the olfactory epithelium. Individual glomeruli in the mammalian main olfactory bulb (MOB) represent a single or, at most, a few types of odorant receptor(s). Signals from different types of receptors are sorted out into different glomeruli. How does the neuronal circuit in the olfactory bulb contribute to the combination and integration of signals received by different glomeruli? Here I examined electrophysiologically whether there were functional interactions between mitral/tufted cells (M/T cells) associated with different glomeruli in the MOB. First, I made simultaneous recordings of extracellular single-unit spike responses of M/T cells and oscillatory local field potentials (OLFPs) in the dorsomedial region of the MOB in urethane-anesthetized rabbits. Using periodic artificial inhalation, the olfactory epithelium was stimulated with a homologous series of *n*-fatty acids or *n*-aliphatic aldehydes. The odor-evoked spike discharges of M/T cells tended to phase-lock to the OLFP, suggesting that spike discharges of many cells occur synchronously during odor stimulation. Second, I made simultaneous recordings of spike discharges from pairs of M/T cells located 300-500 μm apart, and then I performed cross-correlation analyses of their spike discharges in response to odor stimulation. About 27% of cell pairs, which have distinct molecular receptive ranges, exhibited synchronized oscillatory discharges when olfactory epithelium was stimulated with one or a mixture of odorant(s) that were effective in activating both cells. The results suggest that the neuronal circuit in the olfactory bulb causes synchronized spike discharges of specific pairs of M/T cells associated with different glomeruli and the synchronization of odor-evoked spike discharges may contribute to the temporal binding of signals derived from different types of odorant receptor.

Contents

Chapter 1. -General Introduction- 5

Chapter 2. -Materials and Methods- 12

2-1. Animal preparation 13

2-2. Odor stimulation 15

2-3. Recording 17

2-4. Phase-Frequency histogram analysis 18

2-5. Cross-Correlation analysis 20

2-6. Fitting of Gabor functions 21

Chapter 3. -Experiment 1- 23

3-1. Introduction to experiment 1 24

3-2. Spike discharges of M/T cells are phase-locked to the OLFPs 25

Chapter 4. -Experiment 2- 28

4-1. Introduction to experiment 2 29

4-2. Simultaneous recordings of M/T cells innervating with different glomeruli 29

4-3. Cross-correlation analysis 32

4-4. MRR properties and cross-correlograms 34

Chapter 5. -General Discussion- 37

5-1. Comparison to previous reports 38

5-2. Did the pairs of M/T cell recorded innervate different glomeruli? 38

5-3. Possible long range synchronization of M/T cells 39

5-4. Synchronous firing of M/T cells and olfactory cortical neurons 40

5-5. Possible mechanisms to control the synchronization in the MOB 42

5-6. Tuning specificity enhancement by lateral inhibition 43

5-7. Comparison to insect olfactory system 44

References 46

Acknowledgment 55

Chapter 1.

-General Introduction-

Olfactory system is characteristic in that its sensory input is mediated by a variety of odor molecules. It has been estimated that more than 400,000 chemical compounds are odorous to human nose (Hamauzu 1969). Gas-chromatographic studies have shown that an object emits a specific combination of odor molecules, and that different objects emit different combinations of odor molecules. For example, the fruit of peach emits a specific combination of dozens of odor molecules including benzaldehyde and γ-decalactone (Fig. 1). Each of the odor molecules cannot be perceived as "peach" by itself. However, when these odor molecules are mixed in proper concentration, we perceive them as "peach odor". Thus, the olfactory nervous system needs to integrate information carried in a selective combination of odor molecules in order to perceive the "olfactory image" of objects. How does the brain recognize various kinds of odor molecules? What is the neuronal mechanism for the integration of information from various odor molecules?

Odor molecules are received by odorant receptors expressed on the sensory neurons in the olfactory epithelium of the nasal cavity. To cope with a vast variety of odor molecules, the mammalian olfactory system has developed up to 1000 types of odorant receptors (Buck and Axel 1991; Lancet and Ben-Arie 1993; Mombaerts 1999; Sulliavn et al. 1996). One odor molecule can bind to several different odorant receptors, and one odorant receptor can bind to several different odor molecules (Malnic et al. 1999; Zhao et al. 1998). This suggests that a specific combination of odor molecules emitted from an object may activate a specific combination of odorant receptors. The olfactory system may generate the "olfactory image" of object by integrating and/or comparing the information derived from the specific combination

A

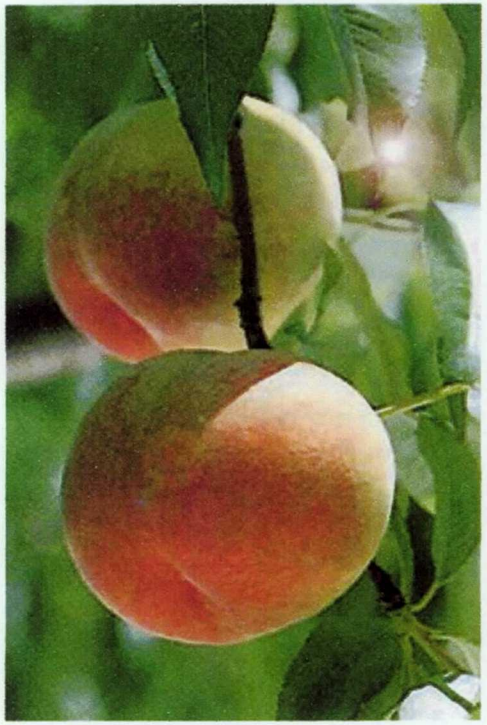

***Prunus Persica Batsch* (Peach)**

B

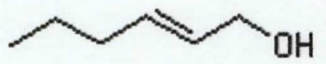

trans-2-hexen-1-ol

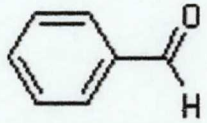

benzaldehyde

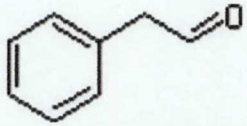

phynylacetoaldehyde

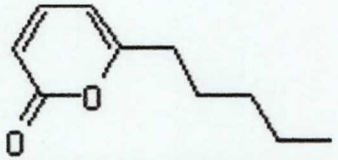

6-pentyl-2-pyrone

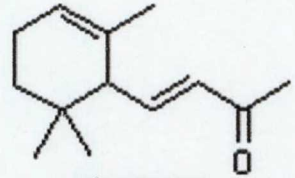

α-ionone

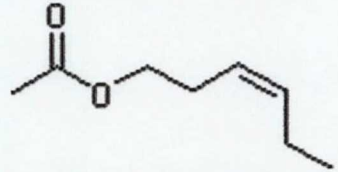

cis-3-hexenyl acetate

γ-decalactone

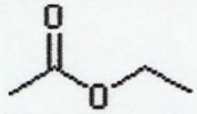

ethyl acetate

Fig. 1 Various kind of odor molecules emitted from the peach fluit. A, a picture of peach (Prunus Persica Batsch). B, 8 odorous compounds emitted from the peach fluit. Except the 8 compoundes above, peach fluits emit various kinds of odorous compounds such as hydrocarbons (ethylene, limonene, etc.), alcohols (ethanol, benzyl alcohol, etc.), acids (acetic acids, hexanoic aicds, etc.), aldehydes (heptanal, turfura, etc.), ketons (2-undecanonde, 2-pyrone, etc.), lactones (γ-octalactone, γ-dodecalactone etc.), esters (isopentyl acetate, benzyl acetate, etc.) and so on.

of odorant receptors.

Individual olfactory sensory neurons express only one type of odorant receptor gene out of a repertoire of 1,000 types of receptor genes (Buck and Axel 1991; Nef et al. 1992; Strotmann et al. 1992; Chess et al. 1994; Malnic et al. 1999). Thus sensory neurons are differentiated into functional subtypes based on the selection of the odorant receptor genes. Individual olfactory sensory neuron projects a single axon to a single glomerulus of the main olfactory bulb (MOB), the first relay station of the central olfactory system. In the glomerulus, olfactory sensory neurons make synaptic connections with the primary dendrites of mitral and tufted cells, which are the principal neurons of the MOB (Fig. 2). The connectivity pattern of olfactory axons to glomeruli is highly organized: individual glomeruli receive converging axonal inputs from olfactory sensory neurons expressing the same type of odorant receptor gene (Mombaerts et al. 1996; Mori et al. 1999). Individual glomeruli thus receive input derived from a given odorant receptor. Therefore signals derived from different odorant receptors are sorted out into different glomeruli (Mori et al. 1999).

How the brain integrates or compare signals derived from different odorant receptors? An olfactory axon makes excitatory synapses to the single primary dendrites of mitral/tufted cells (M/T cells) within a given glomerulus (Fig. 2) (Mori et al. 1983). Therefore, individual M/T cells receive olfactory inputs selectively from sensory neurons expressing a same odorant receptor. It has been estimated in rabbits that about 10 mitral cells and 20 tufted cells associate with one glomerulus (Allison and Warwick 1949; Roeyt et al. 1988). Each glomerulus together with its association neurons can thus form a functional unit, each handling information derived from a single type of odorant

Basic neuronal circuit in the main olfactory system

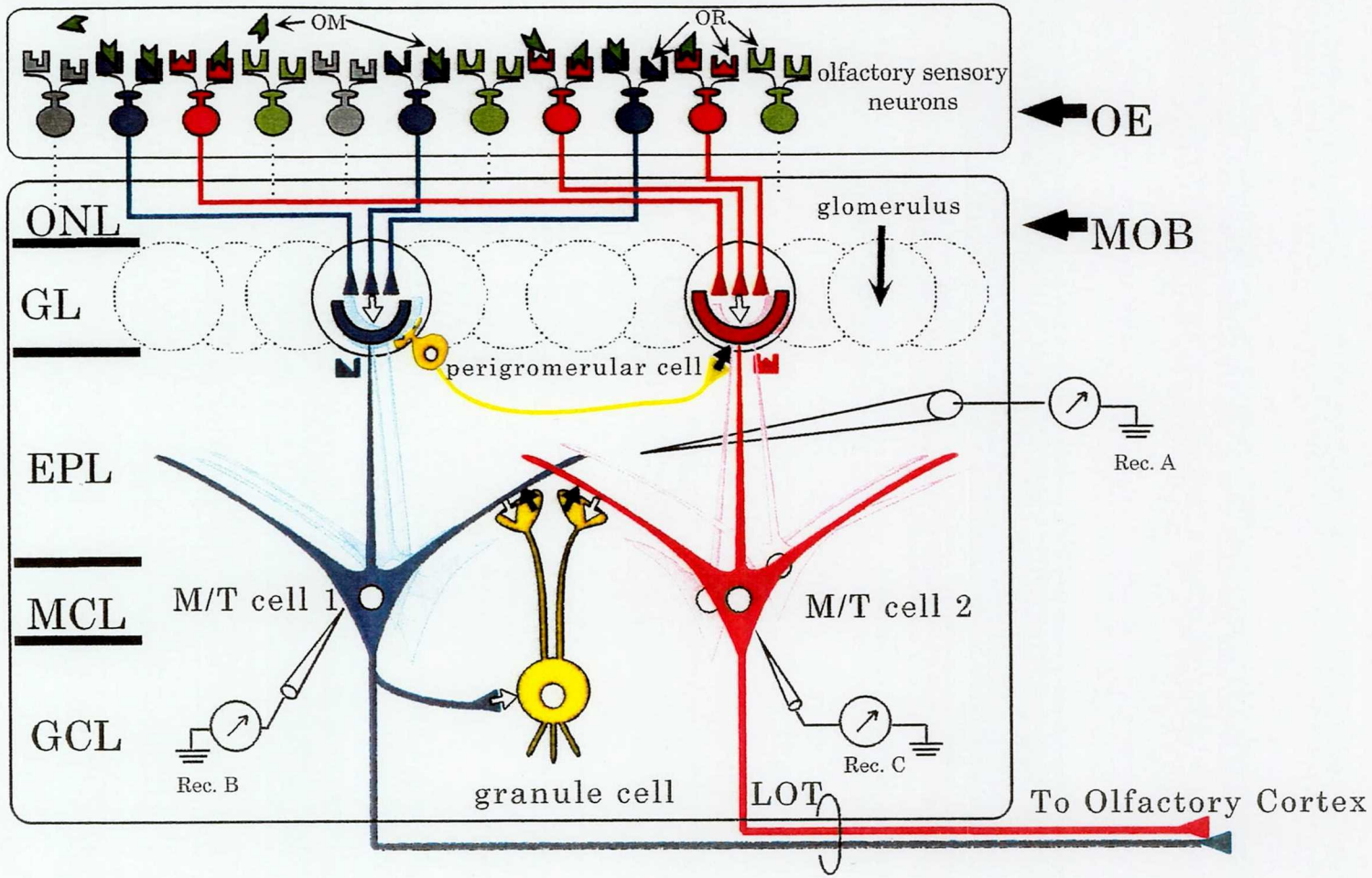

Fig. 2 An over view of the basic neuronal circuit of the mammalian main olfactory system. Olfactory sensory neurons which express the sam odorant receptor gene converge their axons onto a few defined glomeruli and make synaptic connections on dendrites of mitral/tufted cells (M cells) and periglomerular cells. Individual M/T cell project a single primary dendrite to a single glomerulus. M/T cells form dendrodendritic reciprocal synapses with granule cells win the external plexiform layer (EPL), and with periglomerular cells in the glomeruli. White arrows indicate excitatory synapses whereas black ones indicate inhibitory synapses. Oscillatory local field potentials were recorded from EPL (Rec and single unit discharges of M/T cells were recorded from deep EPL or MCL (Rec. B and Rec. C). GCL, granule cell layer; GL, glomerular la er; LOT, lateral olfactory tract; MCL, mitral cell layer; OE, olfactory epithelium; OM, odor molecules; ONL, olfactory nerve layer; OR, odorar receptor.

receptor. It has been suggested that local neuronal circuits within the MOB mediate interactions among different glomerular units.

There are two types of GABAergic interneurons in the MOB, granule cells and periglomerular cells (Fig. 2, Ribak et al. 1977). Granule cells make dendrodendritic reciprocal synapses with M/T cells, thus forming neuronal circuits that may mediate interactions among M/T cells. The dendrodendritic reciprocal synapses consist of the M/T-to-granule excitatory synapse and the granule-to-M/T inhibitory synapse. Thus activation of a M/T cell may activate granule cells via the dendrodendritic excitatory synapses, which then results in inhibition of neighboring M/T cells via the dendrodendritic inhibitory synapses. This lateral inhibition has been suggested to enhance tuning specificity of M/T cells to molecular features of odorants (Yokoi et al. 1995).

Another possible function of the local neuronal circuit might be to meditate the synchronized firing of M/T cells. It has been reported that odor stimulation elicits robust oscillatory local field potentials (OLFPs) in the mammalian MOB. It has been suggested that M/T cells may be tightly coupled with the mechanisms for generating the OLFPs (Adrian 1950; Bressler 1987; Bressler and Freeman 1980; Mori et al. 1992; Mori and Takagi 1977). M/T cells project their axons to olfactory cortical neurons (Shepherd and Greer 1990). If the axons of M/T cells representing different odorant receptors converge onto target neurons in the cortex, the cortical neurons can function as a combination detector whose activity represents the simultaneous activation of the several types of odorant receptors. The synchronized firing of the M/T cells during odor stimulation may effectively drive the target cortical neuron because of the

temporal summation of the excitatory synaptic inputs from the M/T cells.

Synchronous firing of M/T cells in the MOB in response to odor stimulation has already been suggested by the previous studies (Baumgarten et al. 1962, Mori and Takagi 1977, Eeckman and Freeman 1990). However, no systematic study has so far been reported regarding the synchronous firing of M/T cells. In the present study, to examine whether specific pairs of M/T cells representing different odorant receptors show synchronized spike responses when they are co-activated by one or a mixture of odor molecules, I performed the following two experiments.

1. Simultaneous recordings of spike discharges of M/T cell in response to odor stimulation and the OLFP. Detailed analysis was made on the temporal relationship between the time of spike discharges of M/T cells and the phase of the OLFPs.

2. Pair recordings of M/T cells innervating different glomeruli (thus representing different odorant receptors). Cross-correlation analysis was done to test whether the pairs of M/T cells showed synchronized spike responses during specific odor stimulation.

Chapter 2.

-MATERIALS AND METHODS-

2-1. Animal Preparation

Experiments were performed on 17 young adult male rabbits weighing 1.8-2.5 kg (Japanese white, Nihon SLC). Each animal was anesthetized with an intravenous injection (from caudal auricular vein) of 30% urethane (1.3 g/kg). Tracheotomy was performed for double cannulation (Onoda and Mori 1980). A glass canula was inserted caudally into the trachea for animal's spontaneous respiration. A flexible polyethylene tube was inserted rostrally into the postnasal cavity through the larynx for controlling the nasal airflow. Animals were then mounted on a stereotaxic instrument (Narishige, SN-3).

To minimize the pulsation of the brain, a drainage of the cerebrospinal fluid was routinely performed at the atlanto-occipital membrane as followed: after the exposure of the atlanto-occipital membrane, a small hole was opened and a twisted cotton string was inserted through the hole to touch the cerebrospinal fluid. The bone overlying the dorsal surface of the olfactory bulb was widely removed with a dental drill, and the dura was cut and reflected to expose the olfactory bulb. The surface of the olfactory bulb was covered with a mixture of vaseline and mineral oil to reduce drying and cooling.

A small hall was opened in the bone and dura overlying the anterolateral part of the frontal neocortex for inserting a bipolar stimulating electrode into the lateral olfactory tract (LOT) running at the surface of the anterior piriform cortex. The final position of the stimulation electrode was determined by monitoring the LOT-evoked field potentials in the MOB (Phillips et al. 1963). The stimulation electrode was then anchored to the skull with dental cement (Fig. 3).

Animal Preparation

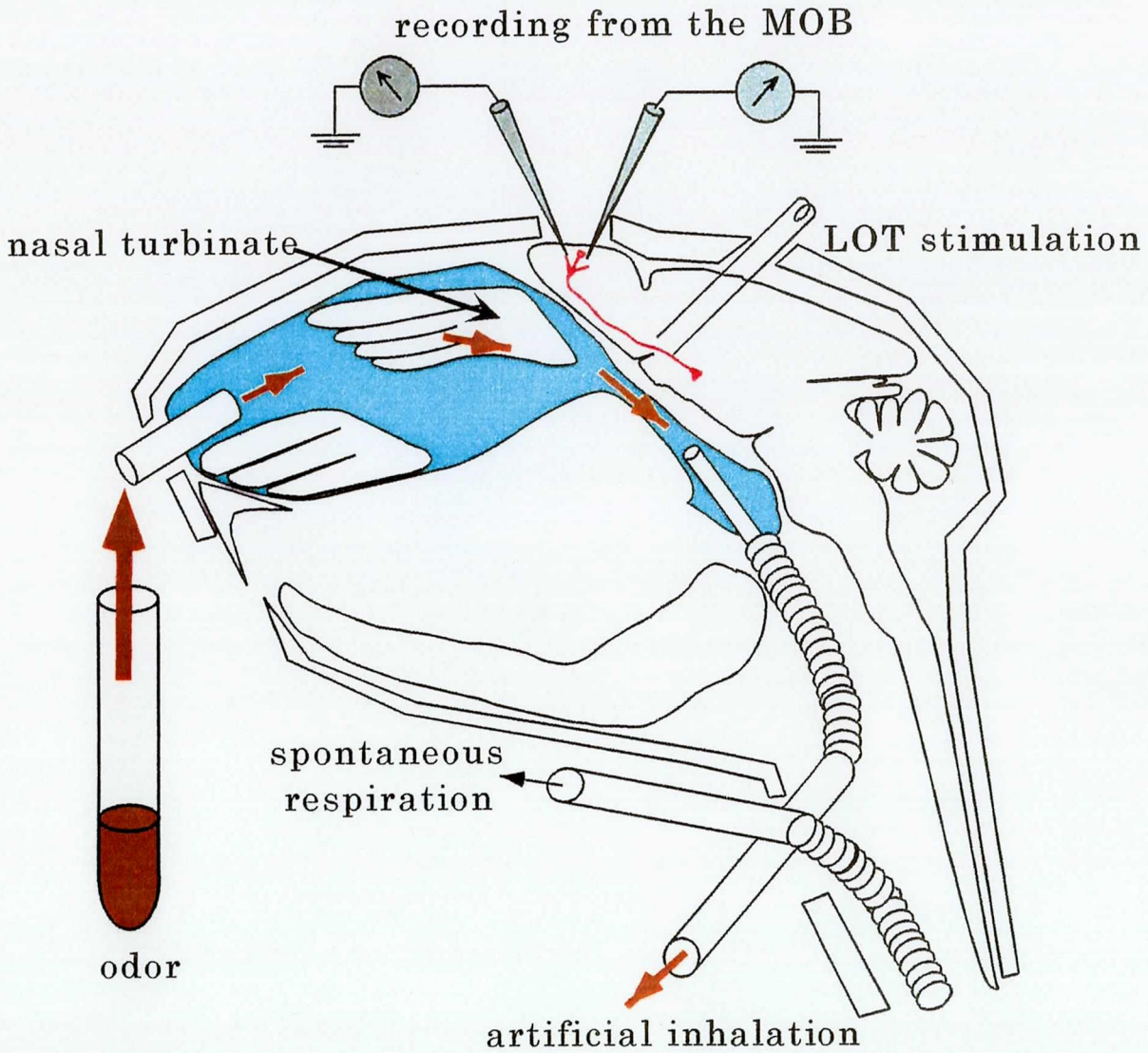

Fig. 3 Animal preparation. After tracheotomy, double canulation was performed: caudal one for respiration and rostral one for artificial inhalation. Orange arrows indicate the flow of odor-containing air during artificial inhalation. Right blue indicates the nasal cavity. A mitral/tufted cells in the MOB is illustrated in red.

2-2. Odor stimulation

A homologous series of *normal-* (*n-*) fatty acids (carbon chain length: 2-9) and *n-* aliphatic aldehydes (carbon chain length: 3-10) were used for odor stimulation (Fig. 4). Each chemical was diluted to 2×10^{-2} (vol/vol) in odorless mineral oil (Aldrich). Two milliliter of each diluted solution was stored in a glass test tube sealed with a screw cap. For odor stimulation, the test tube was uncapped and then placed in front of the animal's nose.

The polyethylene tube inserted rostrally into the postnasal cavity was connected to a vacuum pump for artificial inhalation; the vacuum pump periodically generated negative pressure in the nasal cavity, which caused airflow from the nostril into the nasal cavity. To prevent animals from closing the nostril, a flexible polyethylene tube was inserted into the nostril (Fig. 3). The rate of the artificial inhalation was set as once per 1.5 sec and the duration of one inhalation was 500 msec. By placing the odor-containing test tube in front of the nostril tube, odor-contained air was inhaled into the nasal cavity. Each odor application lasted at least 5 sec covering 3 cycles of the artificial inhalation. To remove the odor-containing air leaked outside the nostril, an air exhauster was placed at a distance of 15 cm from the animal's nose.

Panel of stimulus odor molecules

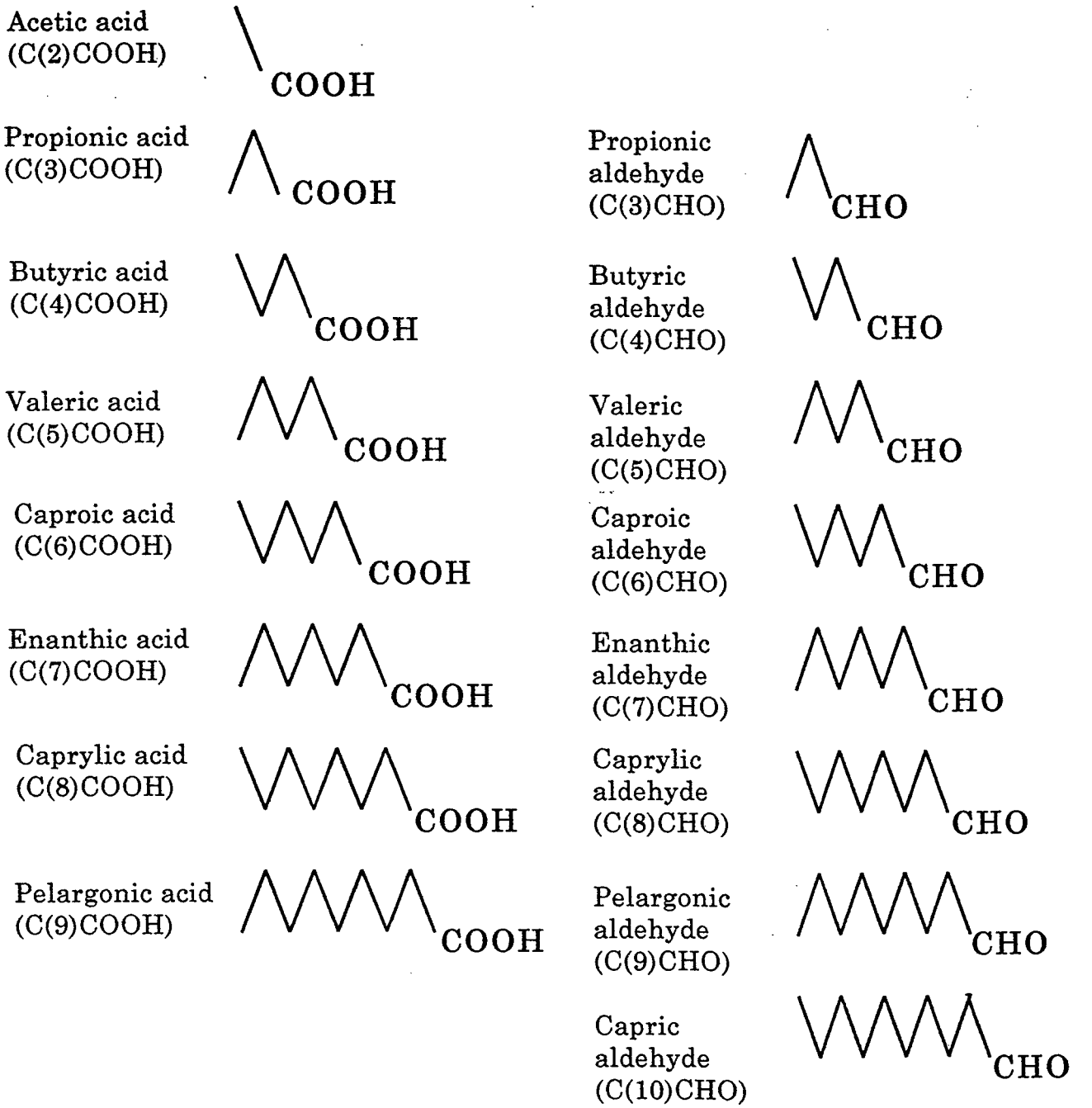

Fig. 4 The panel of odor molecules. *normal* (*n*)- Aliphatic acids (number of carbon atoms: 2-9) and n-aliphatic aldehydes (number of carbon atoms: 3-10) were used. When the olfactory epithelium was stimulated with these odor molecules, mitral/tufted cells in the dorsomedial region of the MOB showed burst spike responses.

2-3. Recording

OLFPs and extracellular single-unit discharges were recorded from the dorsomedial region of the MOB by glass micropipettes filled with 2M NaCl. DC resistance of the micropipettes was 1 - 2 MΩ for the recording of OLFP and 3 - 5 MΩ for the recording of single-unit discharge. Electrical stimulation of the lateral olfactory tract was performed using a rectangular pulse with 100μs duration (Phillips et al. 1963). OLFPs were recorded from the external plexiform layer of the MOB. Single unit discharges of the M/T cells were recorded from the deep portion of the external plexiform layer or the mitral cell layer (Fig. 2). For simultaneous recording of OLFPs and single-unit discharges of a M/T cell, I used two glass micropipettes separated ~100 μm. For simultaneous recording from two M/T cells, the tips of two micropipettes were separated 300 - 500 μm apart. The action potentials and OLFPs were differentially amplified using bandpass filters in the range of 150 Hz - 3 kHz and 5 - 300 Hz, respectively. The recorded signals were stored in the computer (PowerMac 7300, Apple computer) via AD converter Micro 1401 with Spike 2 software (Cambridge Electronic Design, Cambridge) and further off-line analyses were performed.

2-4. Phase-Frequency histogram analysis

To analyze whether spike discharges of M/T cells were phase-locked to the OLFP, I made phase-frequency histograms: time of spike occurrence was plotted against different phases of the sinusoidal OLFP (Laurent et al. 1996).

OLFP was recorded by a micropipette inserted in the middle of the external plexiform layer. One cycle (0°- 360°) of the OLFP was defined as the period from a positive peak (0°) of the sinusoidal OLFP to a next positive peak (360°). To examine the temporal relationship of the spike discharges of M/T cells with reference to the phase of the OLFP, I calculated the phase representation of a spike (λ_{spike}) which is given by:

$$\lambda_{spike} = \left(\frac{t_{spike} - t_{lastOLFPpeak}}{t_{nextOLFPpeak} - t_{lastOLFPpeak}}\right) \times 360$$

where t_{spike} is the time of spike discharges of M/T cell; $t_{lastOLFPpeak}$ is the time of the positive OLFP peak just before the spike discharge; $t_{nextOLFPpeak}$ is the time of the positive OLFP peak just after the spike discharge (Fig. 5). To examine whether spike discharges of M/T cells tend to occur at a restricted phase of the OLFP, a histogram was made by accumulating the occurrence of λ_{spike} in different phases of OLFP (abscissa: phase of the OLFP with 30-degree bins). To show the probability of spike occurrence in each bin, the number of spikes in each bin was divided by the total number of spikes in a histogram.

Phase representation of spike times of M/T cell

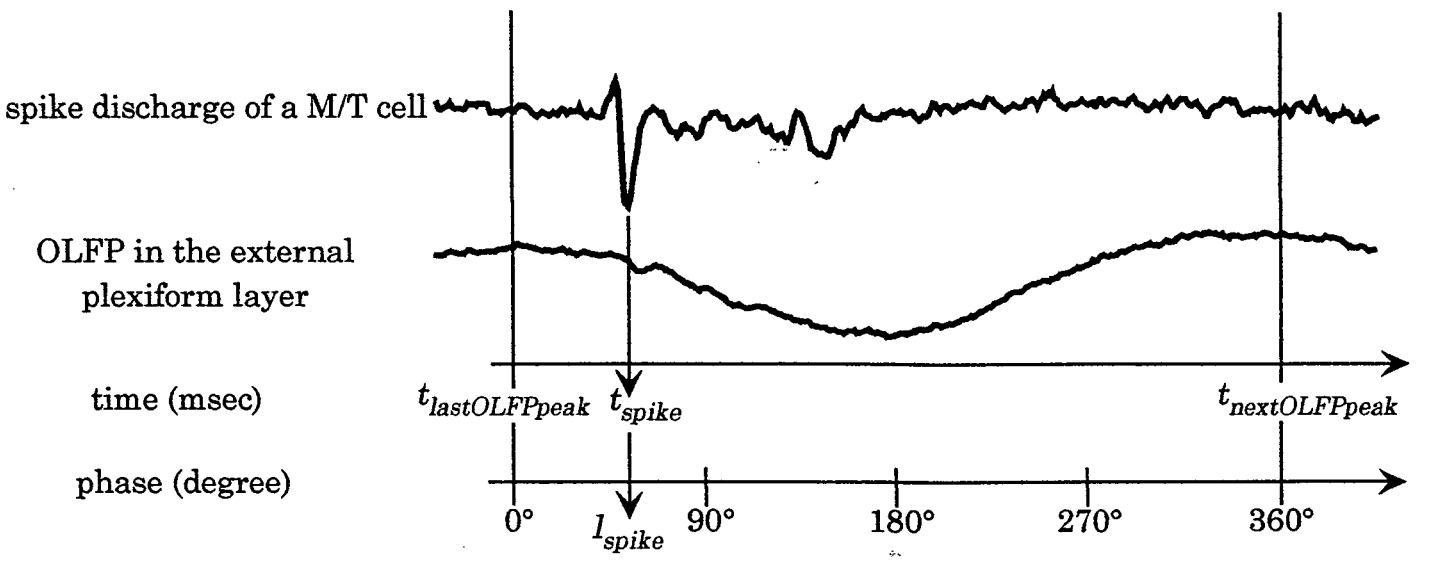

Fig, 5 Representation of spike times of M/T cells in terms of the phase of the OLFP. The interval between two positive peaks of OLFP was regarded as 1 cycle (360 degrees). The time of a spike (t_{spike}) was compared with the last positive peak ($t_{lastOLFPpeak}$) and the next positive peak ($t_{nextOLFPpeak}$) in the simultaneously recorded OLFP and assigned a phase (l_{spike}) by linear interpolation.

2-5. Cross-correlation analysis

To examine the synchrony of spike discharges of a pair of M/T cells, cross-correlation histograms were computed using a standard method (Perkel et al. 1967). Briefly, spike times of cell B with reference to the spike times of cell A were measured and plotted on a histogram. If the two cells show completely synchronized firing, the time lag between spikes of cell A and those of cell B is 0 msec. Thus, the cross-correlogram computed for the completely synchronized spike trains show a clear center peak. If the spikes of cell A occur independently to the spikes of cell B, the cross-correlogram does not show a central peak and is flat. The correlograms were calculated for time shifts ranging from -50 msec to +50 msec with a temporal resolution of 2 msec. I accumulated recordings obtained from at least 3 trials of odor application, each trial consisting of at least 3 artificial inhalations.

2-6. Fitting of Gabor functions

As shown in Fig. 9 and 10, the cross-correlograms that were computed for spike responses of M/T cells often showed a clear central peak and smaller satellite peaks at regular intervals (about 30 msec). To quantify the strength of the cross-correlation, a standard Gabor function (damped sinusoid) was therefore fitted to each cross-correlogram (König 1994). A Gabor function is given by:

$$F(t) = A \cdot \exp\left[-\left(\frac{|t-\theta|}{\sigma}\right)^2\right] \cdot \cos\left[2\pi\nu(t-\theta)\right] + C$$

where A is the center peak amplitude; C is the offset of the correlogram modulation; θ is the phase shift; σ is the decay constant; ν is the sinusoid frequency (see Fig. 6). Each of the five parameters was independently substituted and the Gabor function that fit the correlogram with the lowest χ^2 value is selected (König 1994).

The Gabor function that fit to the cross correlograms had a variable offset (C). Therefore, the relative modulatory amplitude (RMA) defined as the ratio of the center peak amplitude (A) over the offset of correlogram modulation (C) was calculated for assessing the strength of correlation (RMA=A/C, Engel et al. 1990). Spike responses were considered synchronous when the RMA exceeded 0.3.

Parameters of Gabor Function

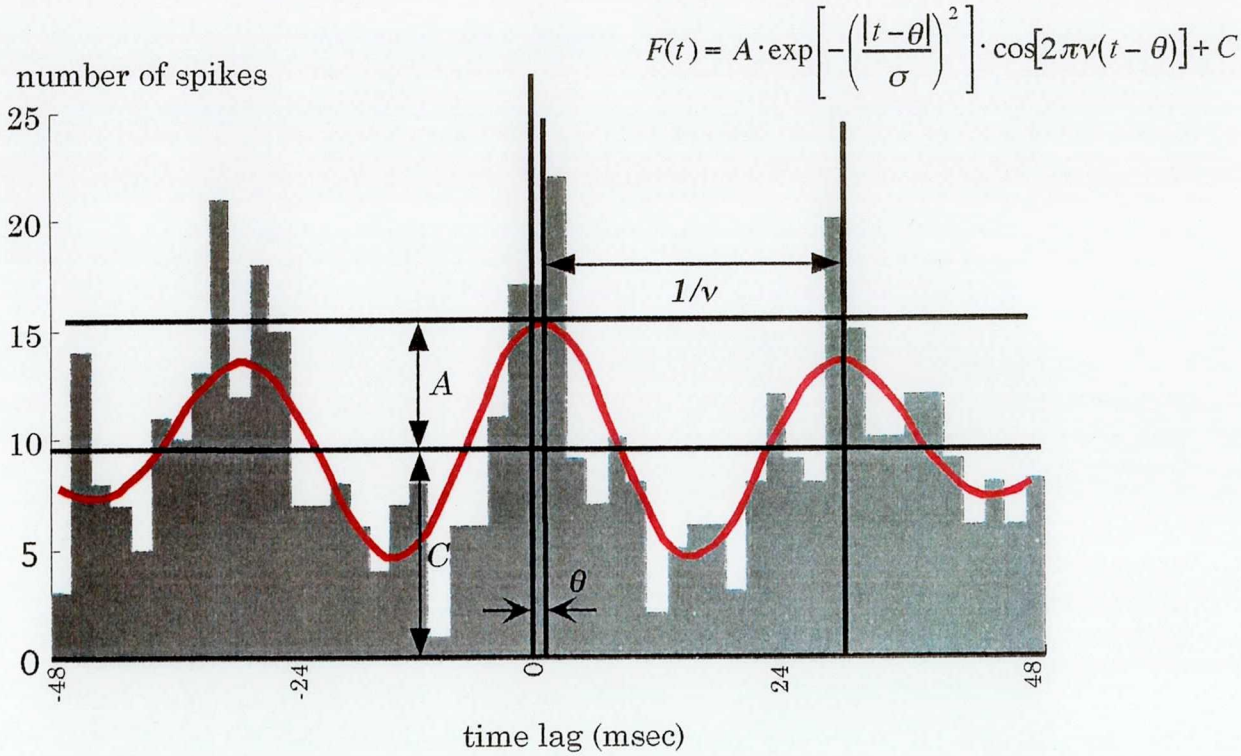

Fig. 6 Fitting a Gabor function (*red*) to a cross-correlogram (gray). Gabor function is the product of the sinusoidal function and the damping function. Each five parameters (C , A, θ, σ, ν) were independently substituted and the fit with the lowest $\chi 2$ value is selected as optimal. σ indicate the decay constant of a function, therefore the bigger σ is, the slower the degree of damping of the function is. A, the center peak amplitude; C, the offset of the correlogram modulation; θ, the phase shift; ν, the sinusoid frequency.

Chapter 3.

-Experiment 1-

3-1. Introduction to experiment 1

Odor stimulation elicits sinusoidal (30-80 Hz) OLFPs in the mammalian MOB (Adrian 1950; Bressler 1987; Bressler and Freeman 1980; Mori et al. 1992; Mori and Takagi 1977). Each type of odor molecules elicits OLFP in specific areas of the MOB. For example, short chain *n*-fatty acids such as propyonic acid elicit OLFPs at restricted regions of the dorsomedial area in the MOB (Mori et al. 1992).

Then, how the odor-induced OLFPs were generated in the MOB? Secondary dendrites of M/T cells make dendrodendritic reciprocal synapses with granule cells in the external plexiform layer of the MOB (Fig. 2). The reciprocal synapses are thought to mediate the OLFP and the synchronized oscillatory activity among many M/T cells (Rall and Shepherd 1968; Rall et al. 1966; Shephered and Greer 1990). It has been proposed the mechanisms eliciting OLFP as follows. Odor-induced activation of M/T cells causes excitation of many granule cells via M/T-to-granule dendrodendritic excitatory synapses. Because the dendrodendritic synapses are located in the external plexiform layer (Fig. 2), the depolarization of granule cell dendrites accompanies the negative extracellular potential in the external plexiform layer. Activation of granule cells, in turn, inhibits many M/T cells simultaneously via granule-to-M/T dendrodendritic inhibitory synapses. When the M/T cells are suppressed, excitatory input to the granule cells subsides. This results in disfacilitation of granule cells followed by a cessation of the inhibition of M/T cells. M/T cells are activated again if excitatory input from olfactory sensory neurons is continued (Mori and Takagi 1977; Rall et al. 1966; Shepherd and Greer 1990).

Previously it was reported that odor-induced spike

responses of mitral cells tended to occur just before the positive peak of the odor-induced OLFPs that were recorded in the granule cell layer (Mori and Takagi 1977). However, the temporal relationship between the spike discharges of mitral cells and the phase of the OLFPs has not yet been examined quantitatively. To examine whether the spike discharges occur at restricted phases of the OLFP during odor stimulation, I performed following two experiments:

1. Simultaneous recordings of OLFP and spike discharges of M/T cells in response to odor stimulation.
2. Quantitative analysis of the temporal relationship between the time of spike discharges of M/T cells and the phase of the OLFPs.

3-2. Spike discharges of M/T cells phase-lock to the OLFPs

To record the odor-induced OLFP, a glass micropipette was inserted into the external plexiform layer (Fig. 2,3) of the dorsomedial fatty-acid responsible region of the MOB (Mori et al. 1992). Another glass micropipette was inserted to record the spike responses of M/T cells (Fig. 2,3). The distance of the two electrodes was set ~100 μm. Fig. 7A exemplifies the simultaneous recordings of OLFP and M/T cell discharges. Odor stimulation (enanthic acid: C(7)COOH) elicited a robust OLFP in the external plexiform layer (*trace 3* of Fig. 7A) and burst spike responses of a M/T cell (*trace 2* of Fig. 7A). The OLFP and the spike discharges occurred during the inhalation of odor-containing air (downward displacement of *trace 1* of Fig. 7A). The spike responses of the M/T cell started before the onset of the robust OLFPs (arrow in Fig. 7A). However, after the onset of the OLFP,

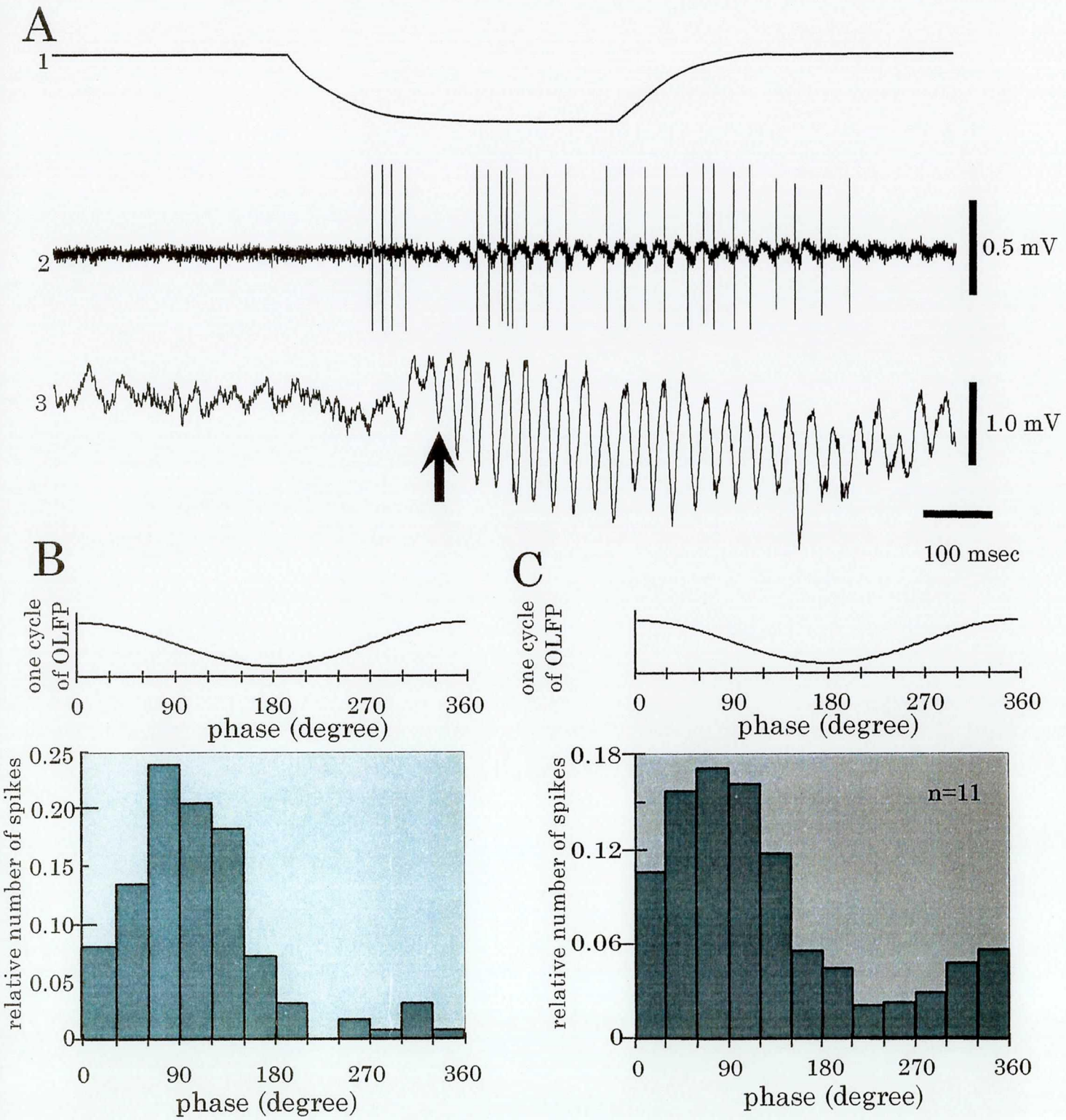

Fig. 7 Spike discharges of M/T cells phase-locked to OLFP. *A:* Simultaneous recordings of single-unit spike responses of a M/T cell (trace 2) and OLFP (trace 3) during odor stimulation. In this case, enanthic acid was applied to the nostril. A monitor for artificial inhalation is shown in trace 1; the downward displacement indicates inhalation. Arrow denotes the onset of the OLFP. B and C. Phase-frequency histograms of spike discharge occurrence plotted against different phases of the sinusoidal OLFP. Each cycle of OLFP was divided into 12 different phases at 30 degree intervals starting from peak of positivity as 0 degree. Upper diagrams in B and C indicate one cycle of OLFP. In B, one cycle of OLFP lasted about 26.6 msec and thus each time bins corresponded to about 2.22 msec. Spike discharges of the M/T cell occurred mostly in the falling phase of the OLFP. C. Average histogram obtained from 11 cells.

spikes of M/T cells occurred in correlation of oscillatory phases of the OLFP. Such a correlation has been observed in all M/T cells examined (n=15).

Next, I examined in detail the temporal relationship between the spikes of M/T cells and the phase of the OLFP (Fig. 5). One cycle of the sinusoidal OLFP was divided into 12 phases and the spike probability of M/T cells in each phase of the OLFPs was examined. Fig. 7B exemplified a phase-frequency histogram. About 91% of spike discharges, which were found during the section robust OLFPs were elicited, occurred during the phases between 0 degree and 180 degree, the falling phase of the OLFPs. The highest spike probability was observed in the phase between 60 to 90 degrees of the OLFP (Fig. 7B).

The preferential occurrence of spike responses during the falling phase of the OLFPs was observed in 11 (about 73%) out of 15 cells examined. In other 4 cells, spike discharges occurred independently to the phase of the OLFPs. Fig. 7C shows an averaged histogram calculated from the data accumulated from the 11 M/T cells. Spikes of M/T cells occurred preferentially during the phases between 0 to 180 degrees of the OLFPs, most frequently between 60 to 90 degrees. Above results indicated that spike responses of many M/T cells was phase-locked to OLFPs during odor stimulation. Thus, it is suggested that many M/T cells fire synchronously during odor stimulation.

Chapter 4.

-Experiment 2-

4-1. Introduction to experiment 2

The results in *Experiment 1* together with previous reports (e. g. Adrian 1950; Bressler and Freeman 1980; Bressler 1987; Mori and Takagi 1977) suggest that many M/T cells may show synchronized spike discharges during odor stimulation. However the phase locking of spikes to OLFP does not necessarily indicate spike synchronization because M/T cells show diverse temporal patterns. To examine the synchronous spike discharges more directly and quantitatively, I made simultaneous recordings from pairs of M/T cells and examined the degree of the synchronization using cross-correlation analysis of their spike discharges. Specific questions asked here are,

1. Do pairs of M/T cells exhibit synchronized spike discharges in response to odor stimulation?
2. Do M/T cells representing different types of odorant receptors show synchronized spike responses?

4-2. Simultaneous recordings of M/T cells innervating different glomeruli

Using a micropipette, I recorded the spike activity of a mitral/tufted cell in the dorsomedial region of the MOB. Then another micropipette was inserted at a distance within 300-500 μm from the first micropipette and recorded spike activity from another M/T cell. Previous studies with horseradish peroxidase labeling showed that cell bodies of almost all pairs of M/T cells innervating a given glomerulus are separated at a distance less than that of an averaged diameter of a glomerulus (Buonviso et al. 1991; Royet et al. 1988, 1989). In rabbit, the average diameter of a glomerulus is about 190 μm (Allison and Warwick

1949). Thus, two M/T cells located at a distance more than 300 μm (about 1.6 times greater than the average diameter) most probably innervate different glomeruli. Mitral cells extend their secondary dendrites tangentially about 850 μm (Mori et al. 1983) so that a pair of mitral cells that are located within 500 μm apart most probably overlap their dendritic field. Based on the above estimation, I aimed to record from two M/T cells located between 300-500 μm apart.

I first examined the response specificity of the pair of M/T cells that was simultaneously recorded and assessed the molecular receptive range (MRR) of each cell (Imamura et al. 1992, Mori and Yoshihara 1995). MRR of a M/T cell reflects strongly the odor-response specificity of the receptor that is represented by the glomerulus that the M/T cell innervates (Mori and Yoshihara 1995). Therefore, if the MRRs of two M/T cells differ, the two M/T cells presumably receive olfactory axon input from different glomeruli. Figure 8 shows an example of simultaneous recording of two M/T cells in the dorsomedial region. When the nasal epithelium was stimulated with caproic acid (C(6)-COOH) (*trace 1* of Fig. 8), both cells showed burst spike discharges (*trace 3* and *4* of Fig. 8) during the inhalation of odor-containing air (downward displacement of *trace 2* of Fig. 8). Observation with a faster sweep of the traces (Fig. 8B) demonstrated that the two cells tended to fire synchronously (indicated by arrows) during the late portion of the burst discharges.

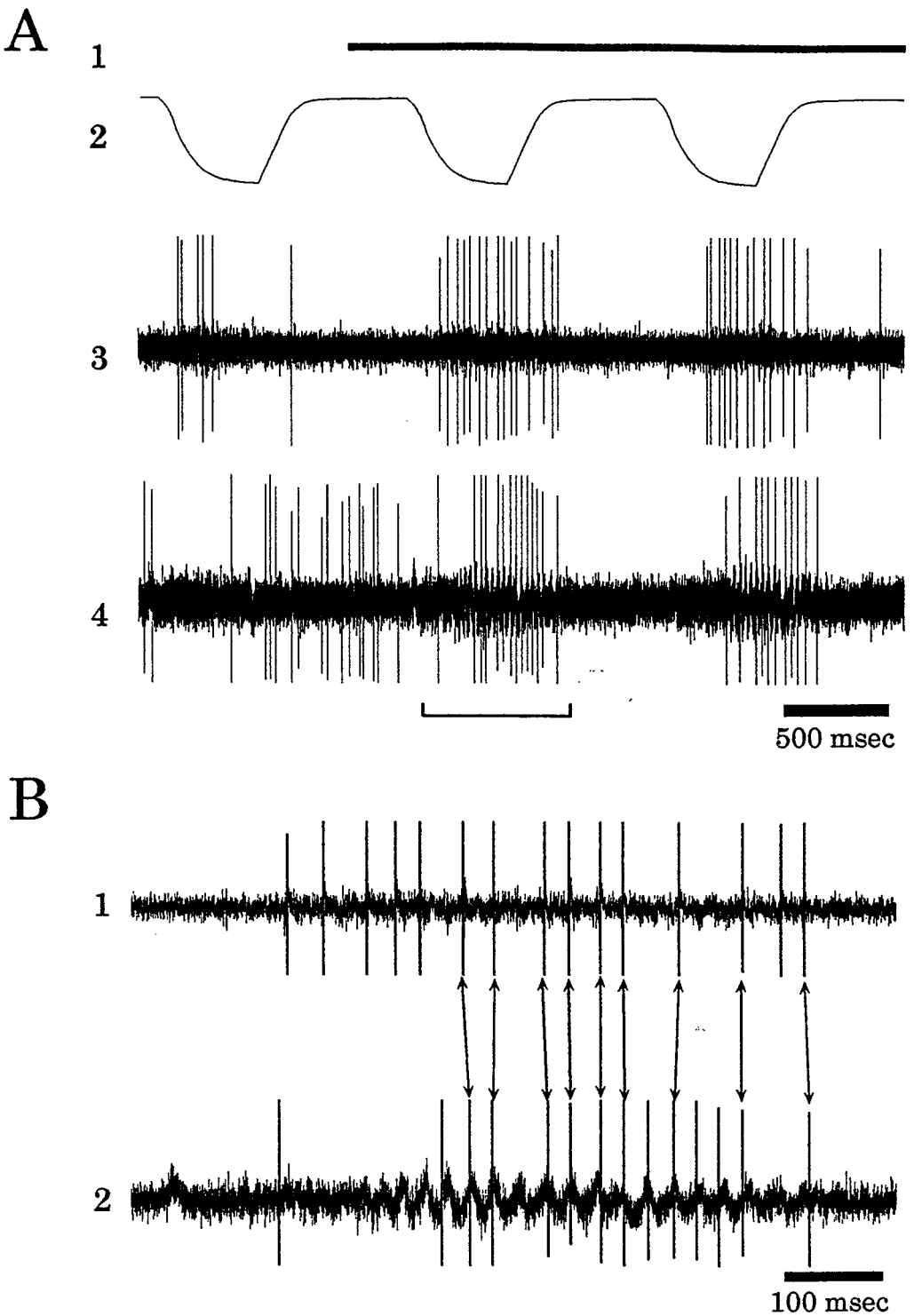

Fig. 8 Simultaneous recording of spike responses of two M/T cells (*trace 3* and *trace 4*). *A:* Thick bar in *trace 1* indicate the period of odor stimulation (caproic acid). Monitor for artificial inhalation is shown in *trace 2*. During the odor-contained air was inhaled into the nostril, both cells showed burst spike responses. *B:* Traces of spike discharges during the period indicated by the bracket under *trace A4* are shown with a faster sweep speed. Spike discharges of these two M/T cells tended to synchronized (arrows) during inhalation of the odor-containing air.

4-3. Cross-correlation analysis

To quantify the synchrony of spike discharges of M/T cells that were simultaneously recorded, I performed cross-correlation analysis to spike trains of pairs of M/T.

Fig. 9 shows an example of the results obtained from simultaneous recordings of two M/T cells. MRR of one cell (S12-2) covered C(3)- and C(4)-fatty acids (COOH) (enclosed by a broken line), while that of the other cell (S12-1) covered C(2)- to C(5)-COOH and C(3)- to C(5)-aliphatic aldehydes (CHO) (enclosed by a solid line) (Fig. 9A). Stimulation of the olfactory epithelium with C(3)-COOH or C(4)-COOH elicited burst spike responses of both cells.

A cross-correlogram calculated for spike trains evoked by C(3)-COOH showed a clear center peak around +3 msec, indicating synchronization. The cell S12-2 fired frequently between 2 msec before and 8 msec after the spike of S12-1. In addition to the center peak, the cross-correlogram had two satellite peaks at -25 msec and +28 msec, indicating that synchronized firing of the two cells occurred periodically (about 36 Hz). It should be noted that the synchronized oscillatory spike discharges appeared only during the inhalation of odor-containing air. There was no apparent correlation in the spontaneous discharges of the cells (Fig. 9C).

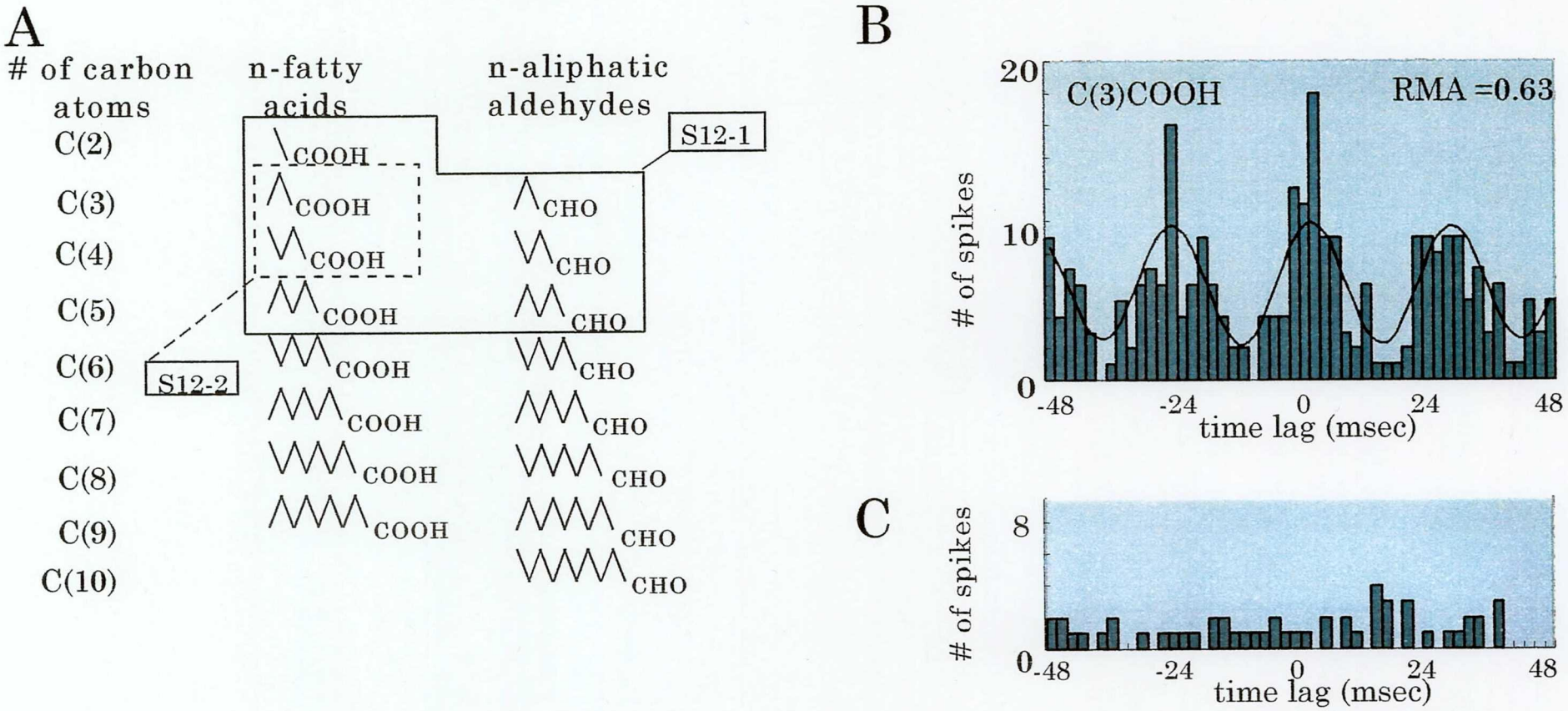

Fig. 9 MRR (*A*) and cross-correlograms (*B* and *C*) of a pair of simultaneously recorded M/T cells (S12-1 and S12-2). *A*: MRRs of the two cells were overlapped at C(3)- and C(4)-COOH. *B*: A cross-correlogram computed for spike discharges evoked by C(3)-COOH. Abscissa indicates the time lag of spike occurrence of cell S12-2 with reference to S12-1. The central peak indicates synchronization. *C*: A cross-correlogram computed for spike discharges recorded before odor stimulation.

4-4. MRR properties and cross-correlograms

In Fig. 9, the MRR of one cell (S12-1) completely covered the MRR of the other cell (S12-2). Therefore, the MRRs of the two cells were different in size but show an intensive overlap. Next, I recorded the pairs of which MRRs were only partially overlapped or not overlapped.

An example obtained from a pair with partially overlapped MRRs is shown in Fig. 10A. In this case, the MRR of S07-1 covered C(2)-, C(3)-, C(4)-, C(5)-, C(6)-COOH and C(3)-, C(4)-CHO whereas the MRR of S07-2 covered C(5)-, C(6)-COOH and C(5)-, C(6)-CHO. Thus, when the nasal epithelium was stimulated with C(5)-COOH or C(6)-COOH, both cells showed spike responses. The cross-correlogram for C(5)-COOH stimulation had a center peak at about -5 msec, indicating synchronization of spikes of both cells with a mean time lag of 5 msec (Fig. 10A). C(6)-COOH stimulation also induced simultaneous activation of both cells but the synchronization was weaker than that for C(5)-COOH stimulation (data not shown).

Fig. 10B demonstrates an example obtained from a pair of M/T cells whose MRR were not overlapped. Cell S26-1 was activated by C(5)-CHO and cell S26-2 was activated by C(7)-CHO and C(8)-CHO. Hence, I could not activate both cells simultaneously with a single chemical compound in the panel of *n*-fatty acid and *n*-aliphatic aldehydes. Therefore a mixture of C(5)-CHO and C(7)-CHO was applied to the nose to activate both cells simultaneously. The top correlogram in Fig. 10B showed a robust synchronization of spike discharges with a mean time lag of 2 msec during the odor stimulation.

In this study, I recorded 195 pairs of M/T cells from the dorsomedial region of the rabbit MOB. In 37 out of them, both

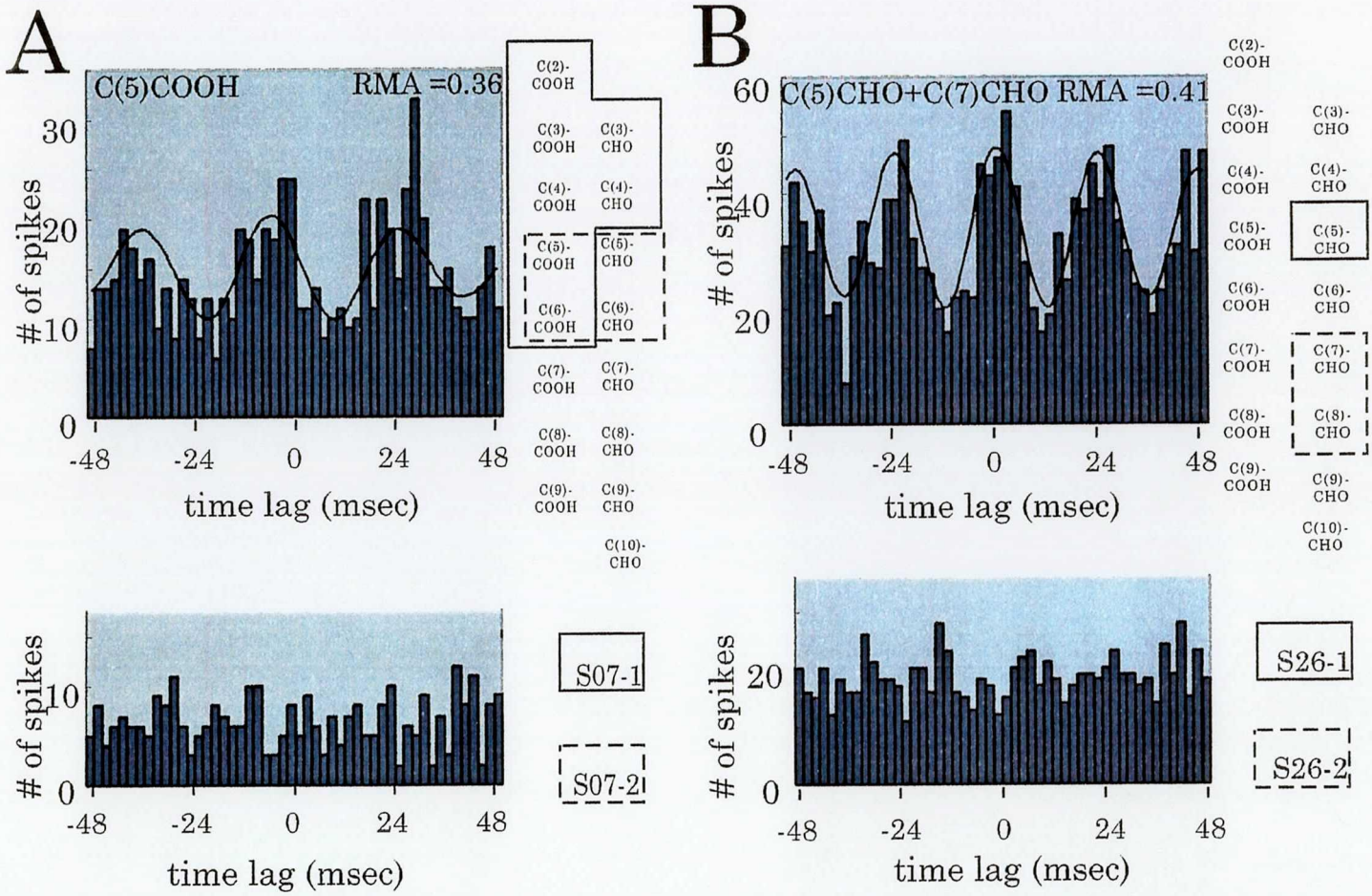

Fig. 10 MRR properties and cross-correlograms of M/T cell pairs. *A*: A pair of M/T cells (S07-1 and S07-2) having distinct but partially overlapping MRRs (*right column*). The cross-correlogram was computed for spike discharges elicited by C(5)-COOH (top panel of *left* column). *B*: Cross-correlogram (*left column*) computed for spike trains in response to a mixture of C(5)-CHO and C(7)-CHO in a pair of M/T cells (S26-1 and S26-2) without overlapping MRRs (*right* column). Lower panels of *left column* in *A* and *B* are cross-correlograms computed for spike trains recorded before odor stimulation.

of the pairs were activated simultaneously with one or mixture of odor molecules. A clear synchronization (RMA>0.3, see MATERIALS AND METHODS and Fig. 6) of spike discharges was observed in 10 pairs (27%). Cross-correlograms obtained from other 27 pairs did not show any clear peaks and the RMAs were smaller than 0.3, indicating that odor stimulation (short carbon chain n-fatty acids or aldehydes) did not induce the synchronized spike discharges of pairs. In all 10 pairs except for one in which the determination of MRR was not completed, the MRR of one cell differed significantly from that of the other cell. In 3 pairs including the pair shown in Fig. 9A, the MRR of one cell was much larger and completely involved that of the other cell. In 4 pairs of M/T cells, the two cells showed distinct but partially overlapping MRRs as exemplified in Fig. 10A. In two pairs of M/T cells, there was no overlap of MRRs (e.g., cell pair shown in Fig. 10B).

In all 10 pairs analyzed, the temporal nature of synchronization was evident: the synchronization was elicited only during the inhalation of odor molecules which activate both cells and no synchronization was observed during the period before the odor stimulation (Fig. 9C and *bottom panels* of Fig. 10A and 10B). These results indicate that when M/T cells receive weak or no sensory inputs, spike discharges of M/T cells do not show synchrony, but once strong sensory inputs come into the MOB, synchronized spike discharges occur among specific combination(s) of M/T cells.

Chapter 5.

-General Discussion-

Present study showed that spike discharges of many M/T cells phase-locked to the OLFP during odor stimulation. This suggests that many M/T cells fire synchronously. Present results also revealed that 10 out of 37 M/T cell pairs located in the dorsomedial region of the MOB, which receive olfactory inputs from different glomeruli, fired synchronously when the effective odorant for both cells were applied.

5-1. Comparison to the previous reports

Previous studies described the relationship between the spike timing of M/T cells and the phases of odor-induced OLFPs (Baumgarten et al. 1962; Mori and Takagi 1977). The membrane potentials of mitral cells oscillated with frequency consisting with that of OLFP (Mori and Takagi 1977). The depolarization of mitral cell membrane is followed by a positive peak of the OLFP recorded in the granule cell layer. It is suggested that the activation of mitral cell leads to the depolarization of granule cell dendrites through the dendrodendritic synapses. Present study extended the previous study and quantitatively analyzed the time lag between mitral cell spike discharges and OLFPs that indicate depolarization of granule cell dendrites.

5-2. Did the pairs of M/T cell recorded innervate different glomeruli?

Because the tips of the two recording microelectrodes were more than 300 μm apart, simultaneously recorded M/T cells presumably innervate different glomeruli. This idea is

supported by the observation that in all pairs, the MRR of one cell differed significantly from that of the other cell. The present results thus suggest that in specific pairs of M/T cells associated with different glomeruli, activation of both cells induces synchronized oscillatory spike discharges during odor stimulation. In view of the evidence that different glomeruli represent different odorant receptors, the results described above suggest that pairs of M/T cells each receiving different odorant receptor inputs show synchronized spike discharges when both receptors are activated by one or a mixture of odor molecules.

5-3. Possible long range synchronization of M/T cells

Dendrodendritic reciprocal synapses between M/T cells and granule cells are thought to be responsible for the synchronized firings of M/T cells. According to the previous report, M/T cells extend their secondary dendrites tangentially about 850 μm (Mori et al 1983), and form extensive dendrodendritic synaptic connections with granule cells. Thus two mitral cells located within 1.7 mm (850 μm ×2) apart, can synchronize their spike discharges through synaptic interactions via granule cells. In addition to the secondary dendrites bridging mediated by granule cells, there is a possible pathway to mediate the synchronized activity of M/T cells. Mitral cells have several axon collaterals in the MOB and make synaptic connections with granule cells (Fig. 2). Average length of axon collaterals of mitral cells is about 1400 μm (Kishi et al. 1984). Therefore, the axon collaterals can propagate the rhythmic activities of M/T cells to granule cells that are located at long distances.

5-4. Synchronous firing of M/T cells and olfactory cortical neurons

I showed that odor stimulation induced the synchronous firing of the M/T cells. Possible function of synchronized spike discharges of the M/T cell is not yet clear. Based on the observations in other sensory systems (e.g. Murthy and Fetz 1996; Singer 1993, 1999; Singer and Gray 1995; Usrey and Reid 1999), however, it can be speculated that synchronous spike responses of M/T cells may provide a basis for the integration of signals derived from different odorant receptors at the level of olfactory cortex (Kashiwadani et al. 1999; Mori et al. 1999). If axons of two M/T cells converge on the same target neuron in the olfactory cortex (Fig. 11), the synchronization of spike discharges may greatly increase the probability of driving the target cortical neuron because of temporal summation of synaptic inputs from the two cells. OLFPs with similar frequencies have been reported in the olfactory cortex (Bressler and Freeman 1980; Bressler et al. 1987), suggesting that synchronized outputs of M/T cells may drive the cortical neurons effectively. Therefore, synchronization of spike discharges of M/T cells may contribute to combining signals derived from different odorant receptors at the level of the olfactory cortex. Extension of the present study to include analysis of olfactory cortical neurons, thus, might provide us with a clue for understanding cellular mechanisms for the integration and decoding in the olfactory cortex of odor information.

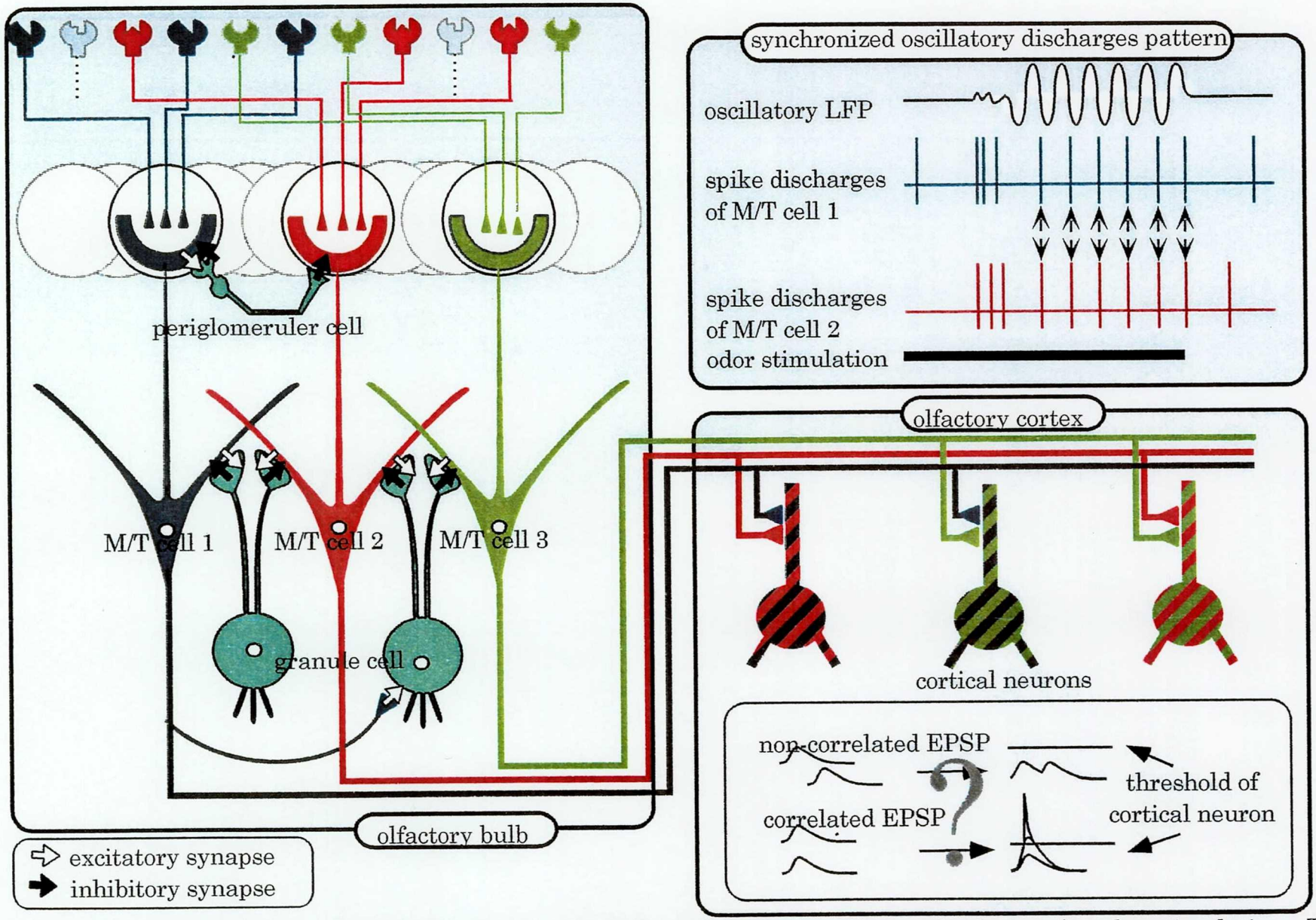

Fig. 11 Summary diagrams. About 1/4 of M/T cell pairs showed synchronized oscillatory discharges by odor stimulation. The synchronized oscillatory spike responses among M/T cells may be mediated by dendrodendritic reciprocal synapses between M/T cell and inhibitory local inter neurons (granule cells and periglomerular cells). If the M/T cells showing synchronized spike responses project their axons onto the same target cortical neurons, synchronized spikes can drive the target neurons effectively and this cortical neuron might play as a combination detector cells.

5-5. Possible mechanisms to control the synchronization in the MOB

Synchronized spike responses of M/T cells are presumably mediated by dendrodendritic reciprocal synapses between M/T cells and inhibitory interneurons such as granule cells and/or periglomerular cells. Interestingly, most of the modulatory centrifugal inputs terminate in the granule cell layer and glomerular layer of the MOB (Shepherd and Greer 1990). Thus, the centrifugal fibers can indirectly affect the local synaptic interactions between the inhibitory neurons and M/T cells.

A subset of pyramidal neurons in the olfactory cortex project back mainly to the granule cells. These feedback inputs are thought to effect the activity of granule cells (Nicoll 1971). Therefore, olfactory cortical neuron may control the activity of the granule cells and thus influence the synchronized spike discharges of M/T cells. In addition to the modulatory inputs from olfactory cortex, other modulatory inputs derived from non-olfactory regions to the MOB may be influenced to the synchronization of M/T cells. These inputs arise from three sources: locus coeruleus (noradrenergic), raphe nuclei (serotonergic), and hind limb of the nucleus of the diagonal band (cholinergic and GABAergic) (Shepherd and Greer 1990; Zaborszky et al. 1986). For example, noradrenergic input from locus coeruleus terminates mainly on the granule cells (McLean et al. 1989). The nature of the physiological actions of noradrenergic input in the MOB is still controversy (Jahr and Nicoll 1982; Jiang et al. 1993; McLennan 1971; Salmoiraghi et al. 1964), however, it might also control the activity of granule cells, and thus the synchronized firing of the M/T cells. Interestingly, noradrenergic inputs are necessary for olfactory memories (Pissonnier et al. 1985; Sullivan et al. 1989), it is possible

that modulation of synchronization of M/T cells by noradrenergic inputs might play some important role for formation of olfactory memories.

5-6. Tuning specificity enhancement by lateral inhibition

In this thesis, I focused on the synchronized oscillatory firing as the functional interaction among M/T cells. Besides the synchronous firing, another type of functional interaction among M/T cells has been known in the MOB: the tuning specificity enhancement by lateral inhibition (Yokoi et al. 1995).

Using a panel of odor molecules with systematic variation in molecular structure, Mori and his colleagues reported that M/T cells show spike responses to a range of odor molecules with similar molecular structure (Imamura et al. 1992; Katoh et al. 1993; Mori et al. 1992). They also reported that inhibitory responses of M/T cells were elicited by odor molecules that have structures similar to those of excitatory odor molecules (Katoh et al. 1993, Yokoi et al. 1995). Because the inhibitory responses are suppressed by the $GABA_A$ receptor antagonist bicuculline in the external plexiform layer, the inhibitory effect seems to be mediated by the GABAergic granule cells (Yokoi et al. 1995). Thus, M/T cells associated with one glomerulus receive lateral inhibition from the M/T cells associating with neighboring glomeruli via dendrodendritic reciprocal synapses. These results suggest that the synaptic interaction may enhance the tuning specificity to odor molecules.

If one glomerulus is strongly activated while another glomerulus is faintly activated, the contrast of the strength of inputs is enhanced by the lateral inhibition. On the contrary,

if two glomeruli are strongly and simultaneously activated, M/T cells associated with the glomeruli may fire synchronously, as shown in the present study.

5-7. Comparison to insect olfactory system

The neuronal circuit in the insect olfactory system resembles that of mammal's (Hildebrand and Shepherd 1997). Olfactory sensory neurons in the antennae project their axons to the glomeruli in the antennal lobe (possible analogue of the olfactory bulb). Projection neurons in the antennal lobe receive inputs from olfactory sensory neurons in several (10-20) glomeruli and project their axons to the mushroom body (possible analogue of the olfactory cortex). In the antennal lobe, projection neurons receive dendrodendritic synaptic input from the local inhibitory GABAergic neurons called local neurons.

Laurent and his colleagues have examined the olfactory system of locusts and bees (Laurent and Naraghi 1994; Laurent and Davidowitz 1994; Laurent et al. 1996; Wehr and Laurent 1996; Macleod and Laurent 1996; Stopfer et al. 1997). When the odor stimulation is applied to the antennae, robust 20-30 Hz oscillatory field potential is induced in the mushroom body (but not in the antennal lobe) (Laurent and Naraghi 1994; Laurent and Davidowitz 1994). The spike responses of the projection neurons were synchronized and phase-locked to the OLFP in the mushroom body (Laurent et al. 1996; Laurent and Davidowitz 1994; Wehr and Laurent 1996). Because the synchronized activity is abolished by picrotoxin (an antagonist of the $GABA_A$ receptor) injected into the antennal lobe, the underlying mechanism may involve GABAergic inhibitory neurons (Macleod and Laurent 1996; Stopfer et al.

1997). Therefore, the mechanisms mediating the synchronized activity of the principal neurons might be similar across the phyla.

Interestingly, applying picrotoxin to the antennal lobe impairs the discrimination of odor molecules with similar molecular structures (Stopfer et al. 1997), raising the possibility that synchronized activity of projection neurons might play a key role for the discrimination between odors. In this paper, however, they cannot exclude the possibility that the change of the tuning specificity of projection neurons by picrotoxin injections may be more effective than desynchronization. Nevertheless, the ideas that synchronized activity of projection neurons may play an important role for integration of signals derived from numerous odorant receptors and for formation of olfactory image of object are still likely. Therefore it is important to further examine whether the synchronized spike activities of M/T cells contribute to the central integration of signals derived from numerous odorant receptors in the mammalian olfactory system.

REFERENCES

ADRIAN, E. D. The electrical activity of the mammalian olfactory bulb. *Electroencephalogr. Clin. Neurophysiol.* 2: 377-388, 1950.

ALLISON, A. C. AND WARWICK, R. T. T. Quantitative observations on the olfactory system of the rabbit. *Brain* 72: 186-197, 1949.

BAUMGARTEN, R. VON., GREEN, J. D., AND MANCIA, M. Slow waves in the olfactory bulb and their relation to unitary discharge. *Electroencephalogr. Clin. Neurophysiol.* 14: 621-634, 1962.

BOEKOFF, I., TAREILUS, E., STROTMANN, J., AND BREER, H. Rapid activation of alternative second messenger pathways in olfactory cilia from rats by different odorants. *EMBO J.* 9: 2453-2458, 1990.

BRESSLER, S. L. Relation of olfactory bulb and cortex I. Spatial variation of bulbocortical interdependence. *Brain Res.* 409: 285-293, 1987.

BRESSLER, S. L. AND FREEMAN, W. J. Frequency analysis of olfactory system EEG in cat, rabbit, and rat. *Electroencephalogr. Clin. Neurophysiol.* 50: 19-24, 1980.

BUCK, L. AND AXEL, R. A novel multigene family may encode odorant receptors: a molecular bases for odor recognition. *Cell* 65: 175-187, 1991.

BUONVISO, N., CHAPUT, M. A., AND SCOTT, J. W. Mitral cell-to glomerulus connectivity: an HRP study of the orientation of mitral cell apical dendrites. *J. Comp. Neurol.* 307: 57-64, 1991.

CHESS, A., SIMON, I., CEDAR, H., AND AXEL, R. Allelic inactivation regulates olfactory receptor gene expression. *Cell* 78: 823-834, 1994.

EECKMAN, F. H. AND FREEMAN, W. J. Correlations between firing and EEG in the rat olfactory system. Brain Research 528: 238-244, 1990.

ENGEL, A. K., KÖNIG, P., GRAY, C. M., AND SINGER, W. Stimulus-dependent neuronal oscillation in cat visual cortex: inter-columnar interaction as determined by cross-correlation analysis. *Eur. J. Neurosci.* 2: 588-606, 1990.

GRAY, C. M., KÖNIG, P., ENGEL, A. K., AND SINGER, W. Oscillatory responses in cat visual cortex exhibit inter-columnar synchronization which reflects global stimulus properties. *Nature* 338: 334-337, 1989.

Hamauzu, Y. Odor perception measurement by the use of odorless room. *Sangyo Kogai* 5: 718-23, 1969.

HILDEBRAND, J. G. AND SHEPHERD G. M. Mechanisms of olfactory discrimination: converging evidence for common principles across phyla. *Ann. Rev. Neurosci.* 20: 595-631, 1997.

IMAMURA, K., MATAGA, N., AND MORI, K. Coding of odor molecules by mitral/tufted cells in rabbit olfactory bulb. I. Aliphatic compounds. *J. Neurophysiol.* 68: 1986-2002, 1992.

JAHR, C. E. AND NICOLL, R. A. Noradrenergic modulation of dendrodendritic inhibition of the olfactory bulb. *Nature* 297: 227-228, 1982.

JIANG, M., GRIFF, E. R., ZIMMER, L. A., ENNIS, M., AND SHIPLEY, M. T. Locus coeruleus increases perithreshold sensor-evoked excitation of mitral cells. *AChemS* 15.

KASHIWADANI, H., SASAKI, Y. F., UCHIDA, N, AND MORI, K. Synchronized oscillatory discharges of mitral/tufted cells with different molecular receptive ranges in the rabbit olfactory bulb. *J. Neurophysiol.* 82: 1786-1792, 1999.

KATOH, K., KOSHIMOTO, H., TANI, A., AND MORI, K. Coding of odor molecules by mitral/tufted cells in rabbit olfactory bulb. II. Aromatic compounds. *J. Neurophysiol.* 70: 2161-2175, 1993.

KISHI, K., MORI, K., AND OJIMA, H. Distribution of local axon collaterals of mitral, displaced mitral, and tufted cells in the rabbit olfactory bulb. *J. Comp. Neurol.* 225: 511-526, 1984.

KÖNIG, P. A method for the quantification of synchrony and oscillatory properties of neuronal activity. *J. Neurosci. Method.* 54: 31-37, 1994.

LANCET, D. AND BEN-ARIE, N. Olfactory receptors. *Curr. Biol.* 3: 668-674, 1993.

LAURENT, G. Dynamical representation of odors by oscillating and evolving neural assemblies. *Trends Neurosci.* 19: 489-496, 1996.

LAURENT, G., WEHR, M., and DAVIDOWITZ, H. Temporal Representation of Odors in an Olfactory Network. *J. Neurosci.* 16: 3837-3847, 1996.

LAURENT, G. AND DAVIDOWITZ, H. Encoding of olfactory information with oscillating neural assemblies. *Science* 265: 1872-1875, 1994.

LAURENT, G. AND NARAGHI, M. Odor-induced oscillations in the mushroom bodies of the locust. *J. Neurosci.* 14: 2993-3004, 1994.

MACLEOD, K. AND LAURENT, G. Distinct mechanisms for synchronization and temporal patterning of odor-encoding neural assemblies. *Science* 274: 976-979, 1996.

MALNIC, B., HIRONO, J., SATO, T., AND BUCK, L. B. Combinatorial receptor codes for odors. *Cell*, 96: 713-723, 1999.

MASTRONARDE, D. N. Correlated firing of cat retinal ganglion cells. I. Spontaneously active inputs to X- and Y cells. *J. Neurophysiol.* 49: 303-324, 1983.

MCLEAN, J. H., SHIPLEY, M. T., NICKELL, W. T., ASTON-JONES, G., AND REVHER, C. K. Chemoanatomical organization of the noradrenergic input form locus coeruleus to the olfactory bulb of the adult rat. *J. Comp. Neurol.* 285: 339-49, 1989.

MCLENNAN, H. The pharmacology of inhibition of mitral cells in the olfactory bulb. *Brain Res.* 29: 177-184, 1971.

MEISTER, M., LAGNADO, L., AND BAYLOR, D. A. Concerted signaling by retinal ganglion cells. *Science*, 270: 1207-1210, 1995.

MOMBAERTS, P., WANG, F., DULAC, C., CHAO, S. K., NEMES, A., MENDELSOHN, M., EDMONDSON, J. AND AXEL, R. Visualizing an olfactory sensory map. *Cell* 87: 675-686, 1996.

MOMBAERTS, P. Molecular biology of odorant receptors in vertebrates. *Annu. Rev. Neurosci.* 22: 487-509, 1999.

MORI, K., KISHI, K., AND OJIMA, H. Distribution of dendrites of mitral, displaced mitral, tufted, and granule cells in the rabbit olfactory bulb. *J. Comp. Neurol.* 219: 339-355, 1983.

MORI, K AND TAKAGI, S. F. Inhibition in the olfactory bulb: dendrodendritic interaction and their relation to the induced

waves. In: *Food Intake and Chemical Senses*, edited by K. Katsuki, M. Sato, S. F. Takagi, and Y. Oomura. Tokyo: Univ. of Tokyo Press, 1977, p. 33-43.

MORI, K., MATAGA, N., AND IMAMURA, K. Differential specificities of single mitral cells in rabbit olfactory bulb for a homologous series of fatty acid odor molecules. *J. Neurophysiol.* 67: 786-789, 1992.

MORI, K., NAGAO, H, AND YOSHIHARA, Y. The olfactory bulb: coding and processing of odor molecule information. *Science* 286: 711-715, 1999.

MORI, K. AND YOSHIHARA, Y. Molecular recognition and olfactory processing in the mammalian olfactory system. *Prog. Neurobiol.* 45: 585-619, 1995.

MURTHY, V. N. AND FETZ, E. E. Synchronization of neurons during local field potential oscillations in sensorymotor cortex of awake monkeys. *J. Neurophysiol.* 76: 3968-3982, 1996.

NEF, P., HERMANS-BORGMEYER, I., ARTIERES-PIN, H., BEASLEY, L., DIONNE, V. E., AND HEINEMANN, S. F. Spatial pattern of receptor expression in the olfactory epithelium. *Proc. Natl. Acad. Sci. U.S.A.* 89: 8948-52, 1992.

NEUENSCHWANDER, S. AND SINGER, W. Long-range synchronization of oscillatory light responses in the cat retina and lateral geniculate nucleus. *Nature* 379: 728-733, 1996.

NICOLL, R. A. Pharmacological evidence for GABA as the transmitter in granule cell inhibition in the olfactory bulb. *Brain Res.* 35: 137-149, 1971.

ONODA, N. AND MORI, K. Depth distribution of temporal firing patterns in olfactory bulb related to air intake cycles. *J.*

Neurophysiol. 44: 29-39, 1980.

PERKEL, D. H., GERSTEIN, G. L., AND MOORE, G. P. Neuronal spike trains and stochastic point processes: II. simultaneous spike trains. *Biophysical J.* 7: 419-440, 1967.

PHILLIPS, C. G., POWELL, T. P. S., AND SHEPHERD, G. M. Response of mitral cells to stimulation of the lateral olfactory tract in rabbit. *J. Physiol.* 168: 65-88, 1963.

PINCHING, A. J. AND POWELL, T. P. S. The neuropil of the glomeruli of the olfactory bulb. *J. Cell Sci.* 9: 347-377, 1971.

PINCHING, A. J. AND POWELL, T. P. S. The neuropil of the periglomerular region of the olfactory bulb. *J. Cell Sci.* 9: 379-409, 1971.

PISSONNIER, D., THIERY, J. C., FABRES-NYS, C., POINDRON, P., AND KEVERNE, E. B. The importance of olfactory bulb noradrenalin for maternal recognition in sheep. *Physiol. Behav.* 35: 361-363, 1985.

RALL, W. AND SHEPHERD, G. M. Theoretical reconstruction of field potentials and dendrodendritic synaptic interactions in olfactory bulb. *J. Neurophysiol.* 31: 884-915, 1968.

RALL, W., SHEPHERD, G. M. REESE, T. S., AND BRIGHTMAN, M. W. Dendrodendritic synaptic pathway for inhibition in the olfactory bulb. *Exp. Neurol.* 14: 44-56, 1966.

ROYET, J. P., SOUCHIER, C., JOURDAN, F., AND PLOYE, H. Morphometric study of the glomerular population in the mouse olfactory bulb: numerical density and size distribution along the rostrocaudal axis. *J. Comp. Neurol.* 270: 559-568, 1988.

ROYET J. P., JOURDAN, F., PLOYE, H., AND SOUCHIER, C.

Morphometric modifications associated with early sensory experience in the rat olfactory bulb: II. Stereological study of the population of olfactory glomeruli. *J. Comp. Neurol.* 289: 594-609, 1989.

REED, R. R. Signaling pathways in odorant detection. *Neuron* 8: 205-209, 1992.

RESSLER, K. J., SULLIVAN, S. L., AND BUCK, L. B. Information coding in the olfactory system: evidence for a stereotyped and highly organized epitope map in the olfactory bulb. *Cell* 79: 1245-1255, 1994.

RIBAK, C. E., VAUGHN, J. E., SAITO, K., BARBER, R., AND ROBERTS, E. Glutamate decarboxylase localization in neurons in the olfactory bulb. *Brain Res.* 126: 1-18, 1977.

ROYET, J. P., SOUCHIER, C., JOURDAN, F., AND PLOYE, H. Morphometric study of the glomerular population in the mouse olfactory bulb: numerical density and size distribution along the rostrocaudal axis. *J. Comp. Neurol.* 270: 559-568, 1988.

ROYET, J. P., JOURDAN, F., PLOYE, H., AND SOUCHIER, C. Morphometric modifications associated with early sensory experience in the rat olfactory bulb: II. stereological study of the population of olfactory glomeruli. *J. Comp. Neurol.* 289: 594-609, 1989.

ROYET J. P., DISTEL, H., HUDSON, R., AND GERVAIS, R. A re-estimation of the number of glomeruli and mitral cells in the olfactory bulb of rabbit. *Brain Res.* 788: 35-42, 1998.

SALMOIRAGHI, G. C., BLOOM, F. E., AND COSTA, E. Adrenergic mechanisms in rabbit olfactory bulb. *Am. J. Physiol.* 207: 1417-1424, 1964.

SHEPHERD, G. M. Discrimination of molecular signals by the olfactory receptor neuron. *Neuron* 13: 771-790, 1994.

SHEPHERD, G. M. AND GREER, C. A. Olfactory bulb. In: *The Synaptic Organization of the Brain.* edited by G. M. Shepherd. New York: Oxford University Press, 1990, p. 139-169.

SINGER, W. Synchronization of cortical activity and its putative role in information processing and learning. *Annu. Rev. Physiol.* 55: 349-374, 1993.

SINGER, W. Neuronal synchrony: a versatile code for the definition of relations? *Neuron* 24: 49-65, 1999.

SINGER, W. AND GRAY, C. M. Visual feature integration and the temporal correlation hypotheses. *Annu. Rev. Neurosci.* 18: 555-586, 1995.

STOPFER, M., BHAGAVAN, S., SMITH, B., AND LAURENT, G. Impaired odour discrimination on desynchronization of odour-encoding neural assemblies. *Nature* 390: 70-74, 1997.

STROTMANN, J., WANNER, I., KRIEGER, J., RAMING, K., AND BREER, H. Expression of odorant receptors in spatially restricted subsets of chemosensory neurons. *Neuroreport* 3: 1053-1056, 1992.

SULLIVAN, R. M., WILSON, D. A., AND LEON, M. Norepinephrine and learning-induced plasticity in infant rat olfactory system. *J. Neurosci.* 9: 3998-4006, 1989.

SULLIVAN, S. L., ADAMSON, M. C. RESSLER, K. J., KOZAK, C. A., AND BUCK, L. B. The chromosomal distribution of mouse odorant receptor genes. *Proc. Natl. Acad. Sci. USA* 93: 884-888, 1996.

TS'O, D. AND GILBERT C. The organization of chromatic and spatial interactions in the primate striate cortex. *J. Neurosci.* 8:

1712-1727, 1988.

USREY, W. M. AND REID, R. C. Synchronous activity in the visual system. *Annu. Rev. Physiol.* 61: 435-456, 1999.

VASSAR, R., CHAO, S. K., SITCHERAN, R., NUÑEZ, J. M., VOSSHALL, L. B., AND AXEL, R. Topographic organization of sensory projections to the olfactory bulb. *Cell* 79: 981-991, 1994.

WEHR, M AND LAURENT, G. Odor encoding by temporal sequences of firing in oscillating neural assemblies. *Nature* 384: 162-166, 1996.

YOKOI, M., MORI, K., AND NAKANISHI, S. Refinement of odor molecule tuning by dendrodendritic synaptic inhibition in the olfactory bulb. *Proc. Natl. Acad. Sci. USA.* 92: 3371-3375, 1995.

ZABORSZKY, L., CARLSEN, J., BRASHEAR, H. R., AND HEIMER, L. Cholinergic and GABAergic afferents to the olfactory bulb in the nucleus of the horizontal limb of the diagonal band. *J. Comp. Neurol.* 243: 488-509, 1986.

ZHAO, H., IVIC, L., OTAKI, J. M., HASHIMOTO, M., MIKOSHIBA, K., AND FIRESTEIN S. Functional expression of a mammalian odorant receptor. *Science* 279: 237-242, 1998.

ACKNOWLEDGMENTS

I am very grateful to Prof. Fujio Murakami, Dr. Nobuhiko Yamamoto and Prof. Kensaku Mori (RIKEN) for giving me a chance to investigate the olfactory system in the Brain Science Institute, RIKEN, for consistent encouragement and for helpful advice to complete this thesis. I wish to great thank to Dr. Yoichi Oda, Prof. Ichiro Fujita and Prof. Takashi Kurahashi for critical reading of this thesis. I would like to express my thanks to Dr. Yasnory F. Sasaki and Dr. Naoshige Uchida for their helpful advice, collaboration and critical discussion. I also thank Drs. Hiroshi Nagao, Lillia Masuda-Nakagawa, Masahiro Yamaguchi, Harald von Campenhausen, Harumi Saito (RIKEN) and Drs. Wen-Jie Song, Hironobu Katsumaru, Hiroaki Kobayashi, Ryuichi Shirasaki (Osaka University) for a number of helpful suggestions, and Ms. Keiko Aijima for her excellent technical assistance. Finally I thank my father Prof. Hiroyuki Kashiwadani and my mother, Harumi Kashiwadani for their continuous encouragement.